LETTER

doi:10.1038/nature14653

Erosion of organic carbon in the Arctic as a geological carbon dioxide sink

Robert G. Hilton[1], Valier Galy[2], Jérôme Gaillardet[3], Mathieu Dellinger[3], Charlotte Bryant[4], Matt O'Regan[5], Darren R. Gröcke[6], Helen Coxall[5], Julien Bouchez[3] & Damien Calmels[7]

Soils of the northern high latitudes store carbon over millennial timescales (thousands of years) and contain approximately double the carbon stock of the atmosphere[1–3]. Warming and associated permafrost thaw can expose soil organic carbon and result in mineralization and carbon dioxide (CO_2) release[4–6]. However, some of this soil organic carbon may be eroded and transferred to rivers[7–9]. If it escapes degradation during river transport and is buried in marine sediments, then it can contribute to a longer-term (more than ten thousand years), geological CO_2 sink[8–10]. Despite this recognition, the erosional flux and fate of particulate organic carbon (POC) in large rivers at high latitudes remains poorly constrained. Here, we quantify the source of POC in the Mackenzie River, the main sediment supplier to the Arctic Ocean[11,12], and assess its flux and fate. We combine measurements of radiocarbon, stable carbon isotopes and element ratios to correct for rock-derived POC[10,13,14]. Our samples reveal that the eroded biospheric POC has resided in the basin for millennia, with a mean radiocarbon age of 5,800 ± 800 years, much older than the POC in large tropical rivers[13,14]. From the measured biospheric POC content and variability in annual sediment yield[15], we calculate a biospheric POC flux of $2.2^{+1.3}_{-0.9}$ teragrams of carbon per year from the Mackenzie River, which is three times the CO_2 drawdown by silicate weathering in this basin[16]. Offshore, we find evidence for efficient terrestrial organic carbon burial over the Holocene period, suggesting that erosion of organic carbon-rich, high-latitude soils may result in an important geological CO_2 sink.

Photosynthesis and the production of organic carbon by the terrestrial biosphere ($OC_{biosphere}$) is a major pathway of atmospheric CO_2 drawdown. Over millennial timescales, some $OC_{biosphere}$ escapes oxidation and contributes to a transient CO_2 sink in soil[2,3,17]. Longer-term CO_2 drawdown can be achieved if $OC_{biosphere}$ is eroded, transferred by rivers and buried in sedimentary basins[9,10,18,19]. Burial of $OC_{biosphere}$ represents a major geological CO_2 sink (and source of oxygen, O_2) alongside the chemical weathering of silicate minerals by carbonic acid, coupled to carbonate precipitation[16,19]. These fluxes negate CO_2 emissions from the solid Earth[20] and from oxidation of rock-derived OC[21], contributing to the long-term regulation of global climate[19,20]. Physical erosion is thought to play an important part in this $OC_{biosphere}$ transfer because it controls the rate of biospheric particulate organic carbon ($POC_{biosphere}$) export by rivers[22,23] and influences sediment accumulation and the efficiency of OC burial[10,18,24].

In the northern high latitudes, large amounts of $OC_{biosphere}$ are stored in soil[1,2]. The upper three metres of soil in the region of northern circumpolar permafrost are estimated to contain 1,035 ± 150 petagrams of carbon (Pg C), approximately double the CO_2 content of the pre-industrial atmosphere[2,17]. Many of these soils accumulated during the retreat of large continental ice sheets following the Last Glacial Maximum, with a peak expansion between 12,000 and 8,000 calibrated years before present (BP)[25], where 'present' is 1950, and the $OC_{biosphere}$ can be thousands of years old[8]. This vast carbon reservoir is located in a region sensitive to environmental change over glacial–interglacial timescales[25] and to warming over the coming century[3]. Much focus has been placed on its potential to become a CO_2 source[3–6,8]. However, geological CO_2 drawdown by $POC_{biosphere}$ erosion at high latitudes has remained poorly constrained[9].

Here we sample POC carried by the major rivers in the Mackenzie basin and investigate its fate using an offshore sediment core extending over the Holocene (Extended Data Fig. 1). The Mackenzie River is the largest source of sediment to the Arctic Ocean[11,12,15] and erosion of mountainous topography in the basin results in a high sediment discharge, similar to the combined total of 16 Eurasian rivers draining to the Arctic Ocean[11,15]. We collected river depth profiles to characterize

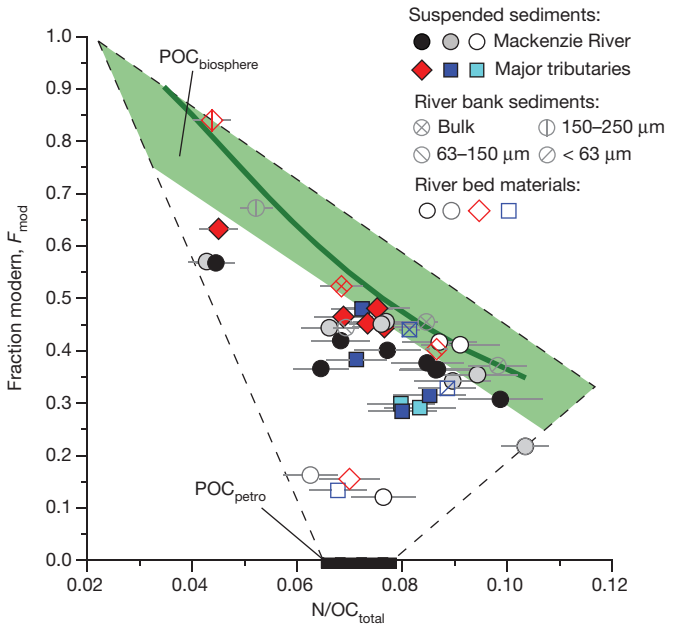

Figure 1 | Source of POC in the Mackenzie River basin. Radiocarbon activity of POC (F_{mod}) versus the nitrogen to organic carbon ratio (N/OC_{total}) of suspended sediments from the Mackenzie River (circles) at the delta (black), at Tsiigehtchic (grey) and at Norman Wells (white) and from its major tributaries the Liard (diamond), the Peel (dark blue square) and the Arctic Red (light blue square). River depth profiles collected in 2010 and 2011 suspended load (filled symbols), river bed materials (open symbols) and sieved bank samples (collected in 2009, sizes shown on figure) are shown with analytical errors (2 standard deviations, s.d.) as grey lines if larger than the data points. The dashed line shows the compositions expected by mixing rock-derived POC_{petro} (black rectangle) and $POC_{biosphere}$ (green shading). The solid green line is the trend from a peat core in western Canada[27].

[1]Department of Geography, Durham University, South Road, Durham DH1 3LE, UK. [2]Department of Marine Chemistry and Geochemistry, Woods Hole Oceanographic Institution, 266 Woods Hole Road, Woods Hole, Massachusetts 02543-1050, USA. [3]Institut de Physique du Globe de Paris, Sorbonne Paris Cité, Universite Paris Diderot, UMR 7154 CNRS, F-75005 Paris, France. [4]NERC Radiocarbon Facility, East Kilbride G75 0QF, UK. [5]Department of Geological Sciences, Stockholm University, Stockholm, SE-106 91, Sweden. [6]Department of Earth Sciences, Durham University, South Road, Durham DH1 3LE, UK. [7]Université Paris-Sud, Laboratoire GEOPS, UMR 8148–CNRS, Orsay, F-91405, France.

©2015 Macmillan Publishers Limited. All rights reserved

POC across the range of grain sizes carried by large rivers[13,14,26] at the main conduit for sediment export to the Arctic Ocean in the Mackenzie delta, at key points on the Mackenzie River and from its major tributaries (Extended Data Fig. 1). To investigate temporal variability of POC composition, river depth profiles were collected shortly after ice break-up at the high/rising stage (June 2011) and during the falling stage (September 2010), while river surface and bank samples were collected in June 2009.

To correct for rock-derived, 'petrogenic' POC (POC_{petro}), likely to be important in the Mackenzie basin[7,26], we combine measurements of radiocarbon (^{14}C, reported as the 'fraction modern', F_{mod}), total OC content ($[OC_{total}]$), stable isotopes of OC ($\delta^{13}C_{org}$), the nitrogen to OC ratio (N/OC_{total}) and the aluminium to OC ratio (Al/OC_{total}), all of which allow us to assess the age and concentration of $POC_{biosphere}$ (see Methods)[7,10,13,14,22,23]. Published ^{14}C ages of surface samples from the Mackenzie River[4,7] ($n = 5$) vary between 6,010 yr and 10,000 yr but the ^{14}C depletion caused by POC_{petro} versus aged $POC_{biosphere}$ has not been assessed. We also examine the hydrodynamic behaviour of POC, using the aluminium-to-silicon ratio (Al/Si) ratio as a proxy of sediment grain size and mineral composition[26].

We find that river POC is depleted in ^{14}C throughout the Mackenzie basin (Extended Data Table 1). F_{mod} values range between 0.28 (^{14}C age 10,106 ± 42 yr) and 0.63 (^{14}C age 3,675 ± 36 yr) in the suspended load ($n = 27$) and between 0.12 (^{14}C age 17,002 ± 84 yr) and 0.16 (^{14}C age 14,601 ± 64 yr) in the river bed materials ($n = 4$). To investigate the cause of this ^{14}C depletion, we examine the N/OC_{total} ratio. Degradation of organic matter in soils can increase the relative N abundance[6,27], differentiating degraded $POC_{biosphere}$ (high N/OC_{total}) from young, fresh $POC_{biosphere}$ (low N/OC_{total}). Suspended load samples display a negative relationship between N/OC_{total} and F_{mod} (Fig. 1), similar to measurements from a peat core in the Mackenzie basin[27] away from permafrost. There, N/OC_{total} ratios increased with ^{14}C age (1,250–10,200 yr) and soil depth (0–3 m). In contrast, river bed materials have lower F_{mod} values and a relatively restricted range of N/OC_{total} values and are distinct from suspended load (Fig. 1). A dominance of POC_{petro} in bed materials[10,14] with a N/OC_{total} ratio of about 0.07 can explain their composition.

Together, the F_{mod} and N/OC_{total} values suggest that POC in the Mackenzie River is a mixture of POC_{petro} and $POC_{biosphere}$, itself varying in ^{14}C age from 'modern' to about 8,000 yr old (Fig. 1). The $\delta^{13}C_{org}$ values and Al/OC_{total} ratios support this inference (Extended Data Fig. 2). Using an endmember mixing analysis[10,13] we quantify POC_{petro} content of sediments (Methods) and find that suspended load at the Mackenzie River delta is dominated by $POC_{biosphere}$ (~70%–90% of the total POC). Having corrected for POC_{petro}, we investigate the source of $POC_{biosphere}$ by estimating its average ^{14}C age. This varies from 3,030 ± 150 yr to 7,900 ± 400 yr (Extended Data Fig. 3) with an average ^{14}C age of $POC_{biosphere}$ = 5,800 ± 800 yr (±2 standard errors, s.e.) in suspended sediments of the Mackenzie River delta. These values are older than estimates of $POC_{biosphere}$ age from the Amazon River (1,120–2,750 yr)[14] and Ganges River (1,600–2,960 yr)[13]. The ages reflect mixing of young, fresh $POC_{biosphere}$ (present in each of these large river basins) with an older $POC_{biosphere}$ in the Mackenzie basin (Fig. 1), likely to consist of peat soils that expanded between 9,000 yr and 8,000 yr (^{14}C age)[25]. $POC_{biosphere}$ can be eroded by slumping and landsliding on river banks, across deep soil profiles[4,7]. Sections of the landscape that have discontinuous permafrost and those undergoing permafrost degradation[28] may be important sources of aged $POC_{biosphere}$, in addition to river banks, which are undercut during peak water discharge following ice break-up[15]. Our samples suggest that erosion and fluvial transfer of millennial-aged $POC_{biosphere}$ is extensive in the Mackenzie basin.

Once in the river, $POC_{biosphere}$ is sorted with river depth, revealed by the Al/Si ratio (Fig. 2b) a proxy for grain size[26]. In bed materials with low Al/Si, POC_{petro} dominates (Fig. 1) and leads to low F_{mod} values (Fig. 2c). Just above the river bed, during the two sampling campaigns, coarse suspended sediments (low Al/Si) hosted the youngest, least degraded $POC_{biosphere}$ (low N/C), leading to a large contrast in ^{14}C age from the bed materials. Towards the river surface, older, more degraded $POC_{biosphere}$ appears to become more dominant, and is transported with fine sediment and clays (high Al/Si)[26]. The large contribution of degraded, very old $POC_{biosphere}$ (>5,000 yr) in the Mackenzie River contrasts with large tropical rivers where organic matter turnover in terrestrial ecosystems is more rapid (Fig. 2c)[13,14].

To assess how erosion in the Mackenzie River may lead to long-term CO_2 drawdown, we estimate $POC_{biosphere}$ discharge. River depth profiles collected at the high and falling stages suggest that the $[OC_{total}]$ of the suspended sediment load did not vary systematically with sediment grain size (Extended Data Fig. 4). Future work should seek to assess temporal variability in POC content and composition. Our data suggest that changes in grain size with water discharge (Fig. 2b) could be important in setting the variability of $POC_{biosphere}$ age carried by the river (Fig. 2c). The $[OC_{total}]$ values at the Mackenzie delta were 1.6 ± 0.5% ($n = 8$, ± 1σ), which were similar to the mean measured in the Mackenzie delta in June–July 1987 of 1.4 ± 0.2 ($n = 10$)[12]. Although our sample set is modest in size, it helps us to better constrain

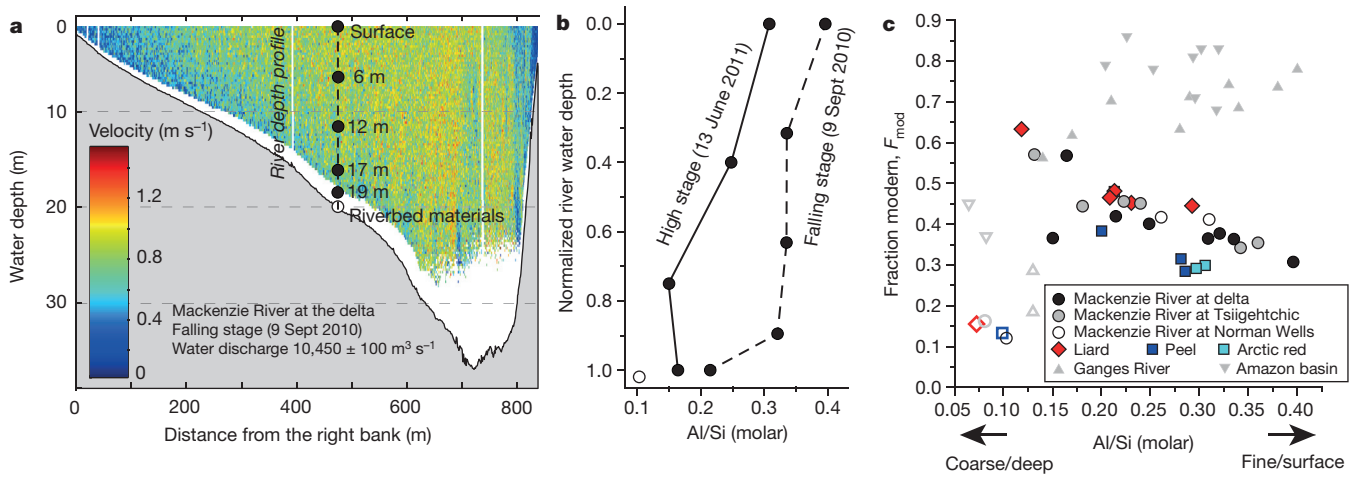

Figure 2 | Transport of POC in the Mackenzie River. **a**, River depth profile collection from the Mackenzie River delta during the falling stage, with Acoustic Doppler Current Profiler data used to determine channel geometry, water velocity and water discharge. **b**, Aluminium to silicon ratio (Al/Si), a proxy for sediment grain size[26], with water depth normalized to maximum depth. Coarser materials are carried throughout the profile during the high stage. **c**, Radiocarbon activity of POC (F_{mod}) versus Al/Si for the Mackenzie basin (this study, symbols as in Fig. 1), Amazon River[14], and Ganges River[10,13]. River suspended load (filled symbols) and river bed materials (open symbols) are distinguished. Analytical errors (2 s.d.) are smaller than the data points.

©2015 Macmillan Publishers Limited. All rights reserved

the range of POC contents in the suspended load of the Mackenzie River. In addition, our endmember mixing analysis allows us to provide the first estimates of [$OC_{biosphere}$], which varies between $0.7 \pm 0.1\%$ and $2.4 \pm 0.2\%$.

To estimate $POC_{biosphere}$ discharge, we use the most complete data set of annual sediment discharge to the Mackenzie delta (1974–1994)[15], which ranged from 81 teragrams per year (Tg yr^{-1}) to 224 Tg yr^{-1}. A Monte Carlo approach is used to account for the modest sample size by using the full measured variability in both [$OC_{biosphere}$] and annual sediment discharge (Methods). We estimate $POC_{biosphere}$ discharge to be $2.2^{+1.3}_{-0.9}$ teragrams of carbon per year (Tg C yr^{-1}), which is sustainable over 1,000 to 10,000 years, depleting the soil carbon stock by ~0.006% per year (Methods). We estimate the POC_{petro} discharge to be $0.4^{+0.1}_{-0.1}$ Tg C yr^{-1}. These estimates do not account for ice-covered conditions, when <10% of the annual sediment discharge is conveyed[12]. Nevertheless, our estimate of $POC_{biosphere}$ discharge is greater than the combined POC discharge of around 1.9 Tg C yr^{-1} by the major Eurasian Arctic rivers (Ob, Yenisei, Lena, Indigirka and Koyma)[11,28] which cover approximately 8.6 million square kilometres. According to the available measurements, the Mackenzie River dominates the input of $POC_{biosphere}$ to the Arctic Ocean.

The mobilization of millennial-aged $POC_{biosphere}$ from soils at high latitudes has been viewed as a short-term source to the atmosphere if decomposition releases greenhouse gases (CH_4 and CO_2)[2–6,8]. However, if $POC_{biosphere}$ escapes oxidation during river transport and is buried offshore, erosion acts as a long-term CO_2 sink[10,18,20,23]. Offshore, aged $POC_{biosphere}$ from the Mackenzie River (Fig. 1) can explain the ^{14}C depletion and $\delta^{13}C$ of bulk organic matter, and old ^{14}C ages of terrestrial plant wax compounds (up to 20,000 yr) in surface sediments of the Beaufort Sea[7,29,30]. We provide new evidence that terrestrial POC is buried efficiently offshore and accumulates in sediments over 10,000 years. Benthic foraminifera ^{14}C ages in a borehole located at the head of the Mackenzie trough (MTW01) indicate that 21 m of sediment have accumulated since $9{,}183^{+125}_{-156}$ calibrated years BP, suggesting a high sedimentation rate during the Holocene of 2.7 ± 0.1 m per thousand years (Extended Data Table 2, Methods). These marine sediments have [OC_{total}] values similar to those measured in the Mackenzie River in both the <63 μm (1.5% to 1.7%) and >63 μm (1.1% to 1.4%) size fractions (Fig. 3). Their N/OC_{total} and $\delta^{13}C_{org}$ values suggest that they are dominated by terrestrial POC with minor marine OC addition (Extended Data Fig. 5). We use the change in OC_{total}/Al ratios offshore to estimate OC burial efficiencies to have been $65 \pm 27\%$ or more over the Holocene at this site (Methods). Rapid sediment accumulation and low temperature are likely to promote high POC burial efficiency[18,23,29]. Also, the fluvial transport dynamics of $POC_{biosphere}$ may promote burial (Fig. 2c). The oldest, most-degraded $POC_{biosphere}$ is transported with clays[26], whose association with organic matter may enhance burial efficiency[18], while the youngest, least-degraded $POC_{biosphere}$ is carried near the river bed at the highest sediment concentrations. Our findings suggest that erosion and riverine transfer at high latitudes can lead to the long-term preservation of terrestrial POC in marine sediments (Fig. 3).

Erosion of high latitude soils and riverine export of $POC_{biosphere}$ may represent an important geological CO_2 sink. Our estimate of the modern day $POC_{biosphere}$ discharge of $2.2^{+1.3}_{-0.9}$ Tg C yr^{-1} in the Mackenzie River may be refined by additional temporal sampling. However, it is three times the modern rates of CO_2 drawdown by weathering of silicate minerals by carbonic acid in the Mackenzie River[16], at around 0.7 Tg C yr^{-1}. Preservation of POC offshore (Fig. 3) suggests that the erosion of high-latitude soils, riverine $POC_{biosphere}$ transport and export to the ocean acts as the largest geological CO_2 sink operating in the Mackenzie basin. We note that these longer-term fluxes are lower than estimates of greenhouse gas emissions from high-latitude soils in permafrost zones, owing to projected warming over the coming century[3,5,6,31]. While these fluxes remain uncertain, recent work[31] has proposed emissions of around 1–2 Pg C yr^{-1} which equate to a yield of

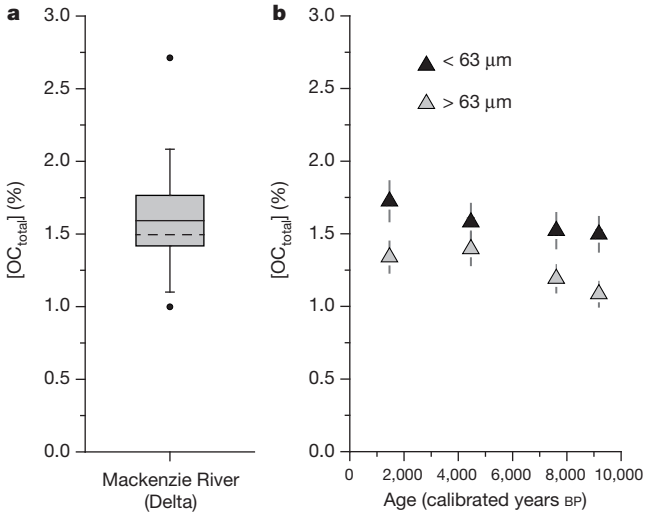

Figure 3 | Fate of particulate organic carbon offshore. **a**, Percentage organic carbon concentration of suspended sediments in the Mackenzie River delta ($n = 8$) where solid line and grey box show the mean ± s.e., whiskers show ±s.d. and the circles indicate the minimum and maximum values. **b**, Percentage $[OC]_{total}$ in sediments <63 μm and >63 μm from core MTW01 in the Mackenzie trough (Extended Data Fig. 1) for depths dated by the ^{14}C activity of mixed benthic foraminifera (Methods), where whiskers show the analytical error if larger than the data point size.

~70 tonnes of carbon per square kilometre per year (t C km^{-2} yr^{-1}) over 17.8×10^8 square kilometres of soils in permafrost zones. This estimate of accelerated release of CO_2 due to anthropogenic warming[31] is more rapid than the natural geological drawdown fluxes, of which we estimate a value for $POC_{biosphere}$ of 2–5 t C km^{-2} yr^{-1} for the Mackenzie basin (Methods). Over longer time periods, we postulate that this geological CO_2 sink may be sensitive to climate conditions in the Arctic. The carbon transfer can operate when high latitudes host substantial $POC_{biosphere}$ stocks in soil, and when rivers can erode and transfer sediments to the Arctic Ocean. Over the last million years, the $POC_{biosphere}$ transfer is likely to have been enhanced during interglacials[25] (Fig. 3), whereas during glacial conditions, lower soil $POC_{biosphere}$ stocks and extensive ice-sheet coverage suggest that $POC_{biosphere}$ erosion may have been suppressed. We propose that erosion of terrestrial $POC_{biosphere}$ by large rivers draining the Arctic could be important in long-term CO_2 drawdown[19,20], coupling the carbon cycle to climatic conditions at high latitudes.

Online Content Methods, along with any additional Extended Data display items and Source Data, are available in the online version of the paper; references unique to these sections appear only in the online paper.

Received 28 August 2014; accepted 3 June 2015.

1. Gorham, E. Northern peatlands: Role in the carbon cycle and probable responses to climatic warming. *Ecol. Appl.* **1,** 182–195 (1991).
2. Hugelius, G. *et al.* Estimated stocks of circumpolar permafrost carbon with quantified uncertainty ranges and identified data gaps. *Biogeosciences* **11,** 6573–6593 (2014).
3. Schuur, E. A. G. *et al.* Vulnerability of permafrost carbon to climate change: Implications for the global carbon cycle. *Bioscience* **58,** 701–714 (2008).
4. Guo, L., Ping, C.-L. & Macdonald, R. W. Mobilization pathways of organic carbon from permafrost to arctic rivers in a changing climate. *Geophys. Res. Lett.* **34,** L13603 (2007).
5. MacDougall, A. H., Avis, C. A. & Weaver, A. L. Significant contribution to climate warming from the permafrost carbon feedback. *Nature Geosci.* **5,** 719–721 (2012).
6. Schädel, C. *et al.* Circumpolar assessment of permafrost C quality and its vulnerability over time using long-term incubation data. *Glob. Change Biol.* **20,** 641–652 (2014).
7. Goñi, M. A., Yunker, M. B., Macdonald, R. W. & Eglinton, T. I. The supply and preservation of ancient and modern components of organic carbon in the Canadian Beaufort Shelf of the Arctic Ocean. *Mar. Chem.* **93,** 53–73 (2005).
8. Vonk, J. E. *et al.* Activation of old carbon by erosion of coastal and subsea permafrost in Arctic Siberia. *Nature* **489,** 137–140 (2012).

©2015 Macmillan Publishers Limited. All rights reserved

9. Vonk, J. E. & Gustafsson, O. Permafrost-carbon complexities. *Nature Geosci.* **6,** 675–676 (2013).
10. Galy, V. *et al.* Efficient organic carbon burial in the Bengal fan sustained by the Himalayan erosional system. *Nature* **450,** 407–410 (2007).
11. Stein, R. & Macdonald, R. W. *The Organic Carbon Cycle in the Arctic Ocean* (Springer, 2004).
12. Macdonald, R. W. *et al.* A sediment and organic carbon budget for the Canadian Beaufort Shelf. *Mar. Geol.* **144,** 255–273 (1998).
13. Galy, V. & Eglinton, T. I. Protracted storage of biospheric carbon in the Ganges-Brahmaputra basin. *Nature Geosci.* **4,** 843–847 (2011).
14. Bouchez, J. *et al.* Source, transport and fluxes of Amazon River particulate organic carbon: insights from river sediment depth-profiles. *Geochim. Cosmochim. Acta* **133,** 280–298 (2014).
15. Carson, M. A., Jasper, J. N. & Conly, F. M. Magnitude and sources of sediment input to the Mackenzie Delta, Northwest Territories, 1974–94. *Arctic* **51,** 116–124 (1998).
16. Gaillardet, J., Dupré, B., Louvat, P. & Allegre, C. A. Global silicate weathering and CO_2 consumption rates deduced from the chemistry of large rivers. *Chem. Geol.* **159,** 3–30 (1999).
17. Sundquist, E. T. & Visser, K. in *Treatise on Geochemistry* (ed. Schlesinger, W. H.), Vol. 8 *Biogeochemistry* 425–472 (Elsevier-Pergamon, 2004).
18. Blair, N. E. & Aller, R. C. The fate of terrestrial organic carbon in the marine environment. *Annu. Rev. Mar. Sci.* **4,** 17.1–17.23 (2012).
19. Hayes, J. M., Strauss, H. & Kaufman, A. J. The abundance of ^{13}C in marine organic matter and isotopic fractionation in the global biogeochemical cycle of carbon during the past 800 Ma. *Chem. Geol.* **161,** 103–125 (1999).
20. Berner, R. A. Atmospheric CO_2 levels over Phanerozoic time. *Science* **249,** 1382–1386 (1990).
21. Hilton, R. G., Gaillardet, J., Calmels, D. & Birck, J. L. Geological respiration of a mountain belt revealed by the trace element rhenium. *Earth Planet. Sci. Lett.* **403,** 27–36 (2014).
22. Hilton, R. G. *et al.* Climatic and geomorphic controls on the erosion of terrestrial biomass from subtropical mountain forest. *Glob. Biogeochem. Cycles* 26**,** http://dx.doi.org/10.1029/2012GB004314 (2012).
23. Galy, V., Peucker-Ehrenbrink, B. & Eglinton, T. Global carbon export from the terrestrial biosphere controlled by erosion. *Nature* **521,** 204–207 (2015).
24. Burdige, D. J. Burial of terrestrial organic matter in marine sediments: a re-assessment. *Glob. Biogeochem. Cycles* **19,** GB4011 (2005).
25. MacDonald, G. M. *et al.* Rapid development of the circumarctic peatland complex and atmospheric CH_4 and CO_2 variations. *Science* **314,** 285–288 (2006).
26. Dellinger, M. *et al.* Lithium isotopes in large rivers reveal the cannibalistic nature of modern continental weathering and erosion. *Earth Planet. Sci. Lett.* **401,** 359–372 (2014).
27. Kuhry, P. & Vitt, D. H. Fossil carbon/nitrogen ratios as a measure of peat decomposition. *Ecology* **77,** 271–275 (1996).
28. Feng, X. *et al.* Differential mobilization of terrestrial carbon pools in Eurasian Arctic river basins. *Proc. Natl Acad. Sci. USA* **110,** 14168–14173 (2013).
29. Goñi, M. A. *et al.* Distribution and sources of organic matter in surface marine sediments across the North American Arctic margin. *J. Geophys. Res.* **118,** 4017–4035 (2013).
30. Drenzek, N. J., Montluçon, D. B., Yunker, M. B., Macdonald, R. W. & Eglinton, T. I. Constraints on the origin of sedimentary organic carbon in the Beaufort Sea from coupled molecular ^{13}C and ^{14}C measurements. *Mar. Chem.* **103,** 146–162 (2007).
31. Schuur, E. A. G. *et al.* Climate change and the permafrost carbon feedback. *Nature* **520,** 171–179 (2015).

Acknowledgements Radiocarbon measurements were funded by the Natural Environment Research Council (NERC), UK (Allocation 1611.0312) to R.G.H and C.B. Fieldwork was funded by CNRS (OXYMORE and CANNIBALT) to J.G. and R.G.H., the Woods Hole Oceanographic Institution Arctic Research Initiative to V.G. and an Early Career Research Grant by the British Society for Geomorphology to R.G.H. V.G. was supported by the US National Science Foundation (OCE-0928582) and H.C. by a Royal Society University Fellowship. The research was carried out under Scientific Research Licence No. 14802 issued by the Aurora Research Centre, who we thank for logistical support (in particular D. Ross and J. Gareis). We also thank I. Peters for preparation of offshore borehole samples, C. Johnson, X. Philippon and M. Bollard for analytical assistance, E. Tipper and K. Hilton for field assistance and discussions and D. Ofukany, G. Lennie, R. Wedel and R. Pilling of Environment Canada for loan of equipment.

Author Contributions R.G.H., V.G. and J.G. conceived the study and R.G.H., J.B., D.C., V.G. and M.D. designed the fieldwork and collected the river samples. M.O. and H.C. collected sediment and carbonate data from the offshore borehole. R.G.H., V.G., M.D., C.B. and D.G. processed the samples and carried out the geochemical analyses. R.G.H. wrote the manuscript with input from all co-authors.

Author Information Reprints and permissions information is available at www.nature.com/reprints. The authors declare no competing financial interests. Readers are welcome to comment on the online version of the paper. Correspondence and requests for materials should be addressed to R.G.H. (r.g.hilton@durham.ac.uk).

©2015 **Macmillan Publishers Limited. All rights reserved**

METHODS

River sample collection and preparation. River depth-profiles from September 2010 and June 2011 (Extended Data Table 1) were used to collect the full range of erosion products and POC in large river systems, taking advantage of the hydrodynamic sorting of particles[10,13,14,26]. At each sampling site (Fig. 1), channel depth, water velocity and instantaneous water discharge were measured by two or more transects with an Acoustic Doppler Current Profiler (ADCP Rio Grande 600 kHz) before each depth profile was collected at a single point (±10 m) in the middle of the channel. On the boat, each sample (~7–8 litres) was evacuated into a clean bucket and stored in sterilized plastic bags and the procedure was repeated depending upon the total water depth. Each bag was weighed to determine the sampled volume, then the entire sample was filtered within 24 h using pre-cleaned Teflon filter units through 90 mm diameter 0.2 µm PES (polyethersulfone) filters[13,26]. Suspended sediment was immediately rinsed from the filter using filtered river water into clean amber-glass vials and kept cool. River bed materials were collected at the base of the depth transects from the boat, using a metal bucket as a dredge, and were decanted to a sterile bag. Riverbank deposits (June 2009) were collected from fresh deposits close to the channel (Extended Data Table 3) and sieved at 250 µm, 150 µm and 63 µm to investigate the sorting of POC[32]. All sediments were freeze-dried upon return to laboratories within two weeks, weighed and homogenized in an agate grinder.

Offshore borehole sample preparation. Marine sediment samples containing benthic foraminifera were obtained from the upper 22 m Holocene sequence of an 85.1-m MTW01 borehole[33] located at 69° 20′ 53′′ N, 137° 59′ 13′′ in 45-m water depth in the Mackenzie trough (Extended Data Fig. 1). Drilled by the Geological Survey of Canada in 1984, the core is currently archived at the GSC-Atlantic core repository. To isolate foraminifera, sediment samples were disaggregated over a sieve with <38 µm mesh using deionized water. On the basis of microfossil counts, four samples were selected with sufficient specimens for radiocarbon dating.

Geochemical analyses. For the river-suspended sediments and core samples for organic carbon analyses, inorganic carbon was removed using a HCl fumigation technique to avoid the loss of a component of POC that is known to occur during a HCl leach[34]. A method adapted to ensure full removal of detrital dolomite was used[35]. In summary, samples were placed in an evacuated desiccator containing about 50 ml 12 N HCl in an oven at between 60 °C and 65 °C for 60–72 h. Samples were then transferred to another vacuum desiccator charged with indicating silica gel, pumped down again and dried to remove HCl fumes. River sediment samples were analysed for organic carbon concentration [OC_{total}] on acidified aliquots and percentage nitrogen concentration [N] on non-acidified aliquots by combustion at 1,020 °C in O_2 using a Costech elemental analyser in Durham. For river depth profile samples, acidified aliquots were prepared to graphite at the NERC Radiocarbon Facility of 1–2 mg C for each sample and standard and ^{14}C was measured by Accelerator Mass Spectrometry at the Scottish Universities Environmental Research Centre and reported as the fraction modern F_{mod} by standard protocol[36]. Process standards (96H humin) and background materials (bituminous coal) were taken through all stages of sample preparation and ^{14}C analysis and were within 2σ uncertainty of expected values. Stable isotopes of POC ($\delta^{13}C_{org}$) were measured by dual-inlet isotope ratio mass spectrometer (IRMS) on an aliquot of the same CO_2. These measurements were consistent with $\delta^{13}C_{org}$ measurements made by an elemental analyser IRMS, normalized to measured standard values ($n = 7$) spanning >30‰ and long-term analytical precision of 0.2‰. Riverbank samples from 2009 were analysed by similar procedures at the National Ocean Sciences Accelerator Mass Spectrometry Facility (NOSAMS) at Woods Hole Oceanographic Institution.

Mixed benthic foraminifera samples chosen from the MTW01 core were analysed at NOSAMS for ^{14}C analyses. Samples were rinsed and no pre-treatments were used. The samples were directly hydrolysed with strong acid (H_3PO_4) to convert the carbon in the sample to CO_2. Calibration of the ^{14}C dates was performed using CALIB (version 7.1)[37]. All ^{14}C dates were normalized to a $\delta^{13}C$ of −25‰ versus VPDB (http://intcal.qub.ac.uk/calib/). Foraminifera dates were calibrated using the MARINE13 data set[38], with a reservoir age correction (ΔR) of 335 ± 85 yr (Extended Data Table 2). The ΔR value is based on a recent reanalysis of ages from 24 living molluscs collected before 1956 from the northwestern Canadian Arctic Archipelago[39]. This calibration set does not include specimens from the Beaufort Sea and as such provides only a best available estimate for ΔR in the Mackenzie trough.

Endmember mixing model. The F_{mod}, N/OC_{total} (Fig. 1), $\delta^{13}C_{org}$ values and Al/OC_{total} values (Extended Data Fig. 2) are consistent with a mixing of POC_{petro} and $POC_{biosphere}$ dominating the bulk geochemical composition of river POC. Autochthonous sources are not an important component based on those measured values, which is consistent with the turbid nature of the Mackenzie River (mean suspended sediment concentration of ~300–400 mg per litre), meaning that like other turbid river systems (for example, the Ganges–Brahmaputra) light penetration is minimal. A mixture of POC_{petro} and $POC_{biosphere}$ can be described by the governing equations[10,13,32]:

$$f_{biosphere} + f_{petro} = 1 \quad (1)$$

$$f_{biosphere} \times \theta_{biosphere} + f_{petro}\theta_{petro} = \theta_{sample} \quad (2)$$

where $f_{biosphere}$ and f_{petro} are the fractions of POC derived from biospheric and petrogenic sources, respectively. θ_{sample} is the measured composition (for example, F_{mod}) of a river POC sample, and $\theta_{biosphere}$ and θ_{petro} are the compositions of biospheric and petrogenic sources. To quantify the f_{petro} in each sample we use the aluminium (Al) to OC_{total} concentration ratio in river sediments. At each locality, a linear trend between F_{mod} and Al/OC_{total} (Extended Data Fig. 2b) can be explained by a mixture of an Al-rich, OC-poor material (rock fragments containing POC_{petro}) with Al-poor, OC-rich material (soils and vegetation debris as $POC_{biosphere}$). Taking advantage of the fact that the POC_{petro} has $F_{mod} \approx 0$ (unmeasurable above the background ^{14}C content), the intercept at $F_{mod} = 0$ gives an estimate of the Al/OC_{total} values and associated uncertainty of the sedimentary rock endmember. To estimate the average concentration of OC_{petro} of bedrocks in each basin, we use the Al concentration of river bed materials as a proxy for the Al concentration in the bedrocks[26] and the Al/OC_{total} value at $F_{mod} \approx 0$. Following previous work in large rivers, we then assume that the OC_{petro} is well mixed in the water column and has a relatively constant [OC_{petro}] value[10,13,14]. This method may overestimate f_{petro} if OC_{petro} has been more extensively oxidized in fine-grained weathering products carried in the suspended load[21]. f_{petro} is quantified using [OC_{petro}] and measured [OC_{total}].

The mixing analysis returns a [OC_{petro}] = 0.12 ± 0.03% (±2σ) in the Liard River and Mackenzie River at Tsiigehtchic, higher values in the Peel River [OC_{petro}] = 0.63 ± 0.30%, with the Mackenzie River at the delta having an intermediate value of [OC_{petro}] = 0.29 ± 0.05%. This is consistent with the known presence of POC_{petro}-bearing sedimentary rocks in the Mackenzie River basin and high OC_{total} contents of bedrocks in the upper Peel River basin and Mackenzie mountains[39]. To quantify the average ^{14}C age of $POC_{biosphere}$ in each sample, equations (1) and (2) can be solved for $\theta_{biosphere}$, using the f_{petro} value and assumed $F_{mod} = 0$ of POC_{petro}. The uncertainty mainly derives from that on f_{petro} and [OC_{total}] and has been propagated through the calculations.

To test whether the mixing of $POC_{biosphere}$ and POC_{petro} can describe the composition of the suspended load samples, we predict the $\delta^{13}C_{org}$ measurements that were not used in the mixing analysis. The calculated f_{petro} values and endmember values of −26.2 ± 0.5‰ for $POC_{biosphere}$ and −28.6 ± 0.5‰ for POC_{petro} were used, informed by measurements of bedrocks[40] and vegetation and soil in the basin[41]. The mixing model (equation (2)) can robustly predict the $\delta^{13}C_{org}$ differences between the Peel and Liard rivers, and between suspended load and bed material $\delta^{13}C_{org}$ values (Extended Data Fig. 2c), supporting a mixing control on the variables.

Mackenzie River POC discharge. To quantify the discharge of POC we need to account for the variability in suspended sediment discharge and the variability in the $POC_{biosphere}$ and POC_{petro} content of sediments in the basin. We use the longest, most complete quantification of sediment flux by the Mackenzie River from 1974–1994 (ref. 15), which has an annual average 127 ± 40 Tg yr^{-1} (±1σ). Annual sediment yield varied from 81 Tg yr^{-1} to 224 Tg yr^{-1}. Although the POC samples were not collected at the same time period, our measurements of [OC_{total}] at the delta (mean 1.6 ± 0.5%; $n = 8$, ±1σ) do not vary systematically between the falling and high stage (Extended Data Fig. 4) and are consistent with available data from samples[12] collected in 1987 (1.4 ± 0.2, $n = 10$).

While future work should aim to constrain the variability in POC composition further, these observations suggest that temporal variability may be less important than the potential variability in [OC_{total}] with depth at a given time, where we find [OC_{total}] values can range from 1.0% to 2.7%. We use our measured range of [$OC_{biosphere}$] and [OC_{petro}] values and the full range of annual sediment yields[15] to quantify $POC_{biosphere}$ and POC_{petro} discharge and the associated uncertainty using a Monte Carlo approach. Over 100,000 simulations, we use a 'flat' probability for the range of values for both variables (that is, equal probability of all measured values). This allows us to fully explore the range of estimates given the available measurements. Future work seeking to expand the number of [$OC_{biosphere}$] measurements to assess its flux-weighted mean and variability, while assessing temporal variability in more detail, will allow POC discharge estimates and their uncertainty to be refined. $POC_{biosphere}$ ($2.2^{+1.3}_{-0.9}$ Tg C yr^{-1}) and POC_{petro} ($0.4^{+0.1}_{-0.1}$ Tg C yr^{-1}) discharges are reported as the median (50%) ± 1 s.d. Over the sediment source areas of the Mackenzie (downstream of the Great Slave Lake[15]) of 774,200 km^2, these equate to yields of $POC_{biosphere} = 2.9^{+1.7}_{-1.1}$ t C km^{-2} yr^{-1} and $POC_{petro} = 0.6^{+0.2}_{-0.2}$ t C km^{-2} yr^{-1}.

©2015 Macmillan Publishers Limited. All rights reserved

The total POC discharge is slightly higher than a previous estimate ($2.1\ Tg\ C\ yr^{-1}$)[12] based on measurements of POC content made in 1987 because: (1) we account for higher $POC_{biosphere}$ concentrations which may occur in water-logged $POC_{biosphere}$ near the river bed (Fig. 2c, Extended Data Fig. 4); and (2) we account for the potential for very high annual sediment discharge[15]. Based on estimates of soil carbon stock in the Mackenzie basin[2] of $\sim 50 \times 10^3\ t\ C\ km^{-2}$ and the upstream sediment source area (downstream of the Great Slave Lake, 774,200 km^2), the present rate of $POC_{biosphere}$ export represents a depletion of the soil carbon stock by ~0.006% per year, which is sustainable over 1,000 to 10,000 years.

OC burial efficiency in MTW01. To estimate the burial efficiency of terrestrial POC at the MTW01 site, we normalize the measured [OC_{total}] concentrations (Fig. 3) by Al concentration; Al is an immobile inorganic element hosted by major mineral phases. The OC_{total}/Al normalization allows the effects of dilution to be distinguished from net OC gain (increased ratio) or OC loss (decreased ratio). The mean OC_{total}/Al of the MTW01 samples was 0.17 ± 0.02 g C per g Al ($n = 4, \pm 2$ s.e.). This is lower than the mean OC_{total}/Al of the suspended load samples from the Mackenzie River delta of 0.26 ± 0.10 g C per g Al ($n = 8, \pm 2$ s.e.). The decrease in the ratio offshore may suggest a higher relative proportion of POC_{petro} (Extended Data Fig. 2b); however, this is not consistent with the less negative $\delta^{13}C_{org}$ values (Extended Data Fig. 5). The decrease can therefore be interpreted in terms of OC loss, with the ratio of core to river samples being $0.17 \pm 0.02/0.26 \pm 0.10$.

Assuming that all the change in OC_{total}/Al is driven by OC loss, and taking into account the measurement variability in these values, we estimate that $65 \pm 27\%$ of the OC has been preserved. However, we note that the OC_{total}/Al ratios in the core are not statistically different from the river suspended load samples (one-way ANOVA, $P > 0.1$) which suggests that the OC burial efficiency could be higher (that is, 100%). In addition, if we use the OC_{total}/Al of finer river sediments carried near the channel surface—which may be more easily conveyed offshore—of $0.20 \pm 0.04\ g\ g^{-1}$ ($n = 4, \pm 2$ s.e.), we calculate burial efficiency to be $85 \pm 20\%$. Future work should seek to better constrain these burial efficiencies with additional terrestrial and marine samples. Nevertheless, despite the remaining uncertainty, these high burial efficiencies[18] are consistent with the high sedimentation rate and low temperature setting. The long-term burial of POC delivered to sites deeper in the Beaufort Sea[29] still remains to be assessed to provide a complete picture of source-to-sink carbon transfers.

32. Hilton, R. G., Galy, A., Hovius, N., Horng, M. J. & Chen, H. The isotopic composition of particulate organic carbon in mountain rivers of Taiwan. *Geochim. Cosmochim. Acta* **74,** 3164–3181 (2010).
33. Moran, K., Hill, P. R. & Blasco, S. M. Interpretation of piezocone penetrometer profiles in sediment from the Mackenzie Trough, Canadian Beaufort Sea. *J. Sedim. Petrol.* **59,** 88–97 (1989).
34. Komada, T., Anderson, M. R. & Dorfmeier, C. L. Carbonate removal from coastal sediments for the determination of organic carbon and its isotopic signatures, ^{13}C and ^{14}C: comparison of fumigation and direct acidification by hydrochloric acid. *Limnol. Oceanogr.* **6,** 254–262 (2008).
35. Whiteside, J. H. *et al.* Pangean great lake paleoecology on the cusp of the end-Triassic extinction. *Palaeogeogr. Palaeoclimatol. Palaeoecol.* **301,** 1–17 (2011).
36. Stuiver, M. & Polach, H. A. Discussion: Reporting of ^{14}C data. *Radiocarbon* **19,** 55–63 (1977).
37. Stuiver, M. & Reimer, P. J. Extended ^{14}C database and revised CALIB radiocarbon calibration program. *Radiocarbon* **35,** 215–230 (1993).
38. Reimer, P. J. *et al.* IntCal09 and Marine09 radiocarbon age calibration curves, 0–50,000 years cal BP. *Radiocarbon* **51,** 1111–1150 (2009).
39. Coulthard, R. D., Furze, M. F. A., Pienkowski, A. J., Nixon, F. C. & England, J. H. New marine ΔR values for Arctic Canada. *Quat. Geochronol.* **5,** 419–434 (2010).
40. Johnston, D. T., Macdonald, F. A., Gill, B. C., Hoffman, P. F. & Schrag, D. P. Uncovering the Neoproterozoic carbon cycle. *Nature* **483,** 320–323 (2012).
41. Bird, M., Santruckova, H., Lloyd, J. & Lawson, E. The isotopic composition of soil organic carbon on a north-south transect in western Canada. *Eur. J. Soil Sci.* **53,** 393–403 (2002).
42. Brown, J. *et al. Circum-Arctic Map of Permafrost and Ground Ice Conditions* http://nsidc.org/data/ggd318 (National Snow and Ice Data Center/World Data Center for Glaciology, 1998).

©2015 Macmillan Publishers Limited. All rights reserved

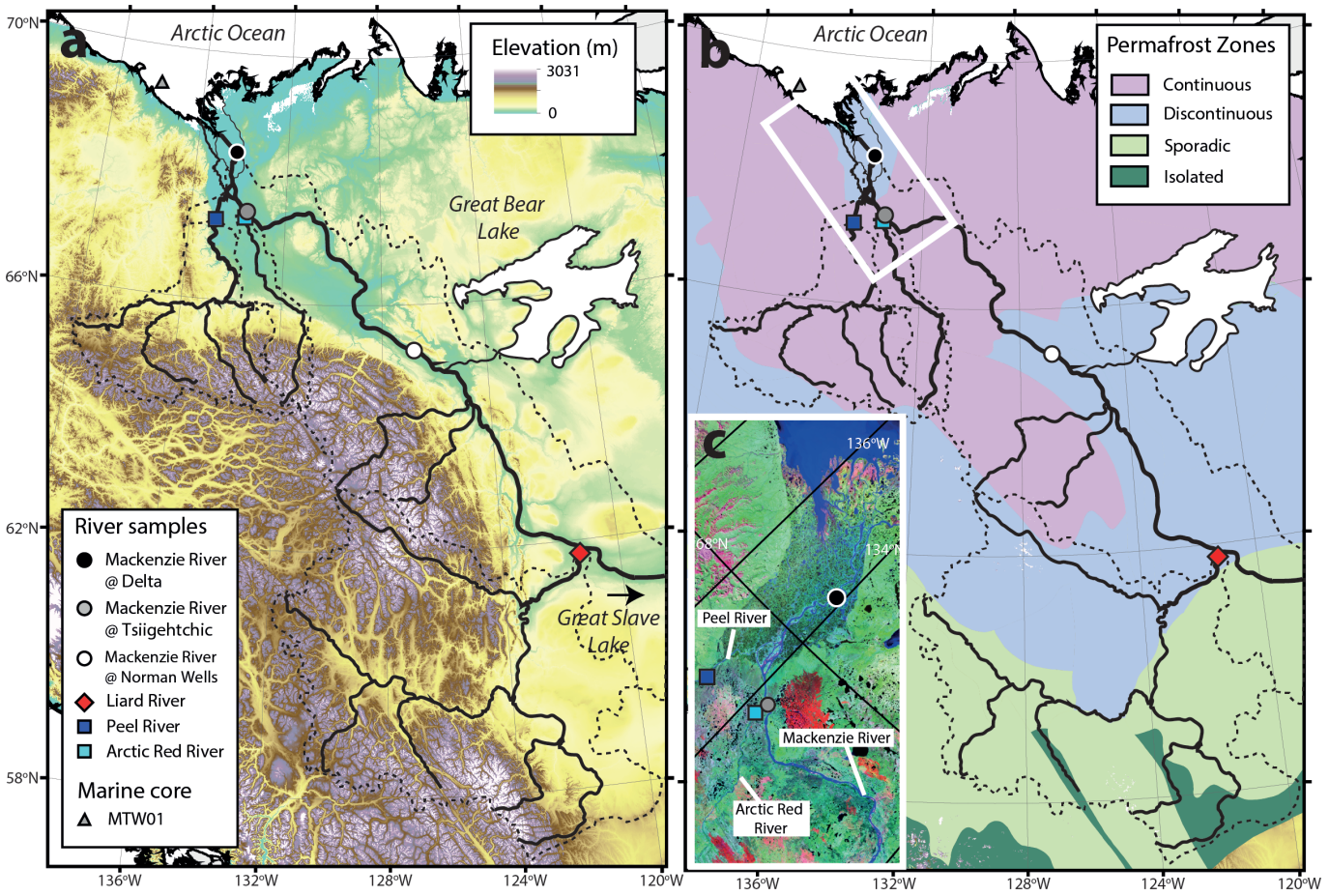

Extended Data Figure 1 | The location of river depth profiles collected from the Mackenzie River. Three locations along the Mackenzie River were sampled (circles) at the delta (black), Tsiigehtchic (grey) and Norman Wells (white) in addition to the major tributaries, the Liard River (red diamond), Arctic Red River (light blue square) and Peel River (dark blue square). The location of the sediment core MTW01 from the Mackenzie trough is shown (triangle). **a**, Major river channels (black lines) overlain on digital elevation model GMTED 15 arcsec with upstream sediment source catchment areas delineated by flow accumulation and flow direction outputs from the digital elevation model (dotted lines). The Great Slave Lake is indicated upstream of the Liard confluence and acts as an effective sediment trap in the basin[15]. **b**, Permafrost zone coverage in the upstream areas of the basin[42]. White rectangle shows the sample locations near the Mackenzie delta displayed in **c**, overlain on LANDSAT imagery.

©2015 Macmillan Publishers Limited. All rights reserved

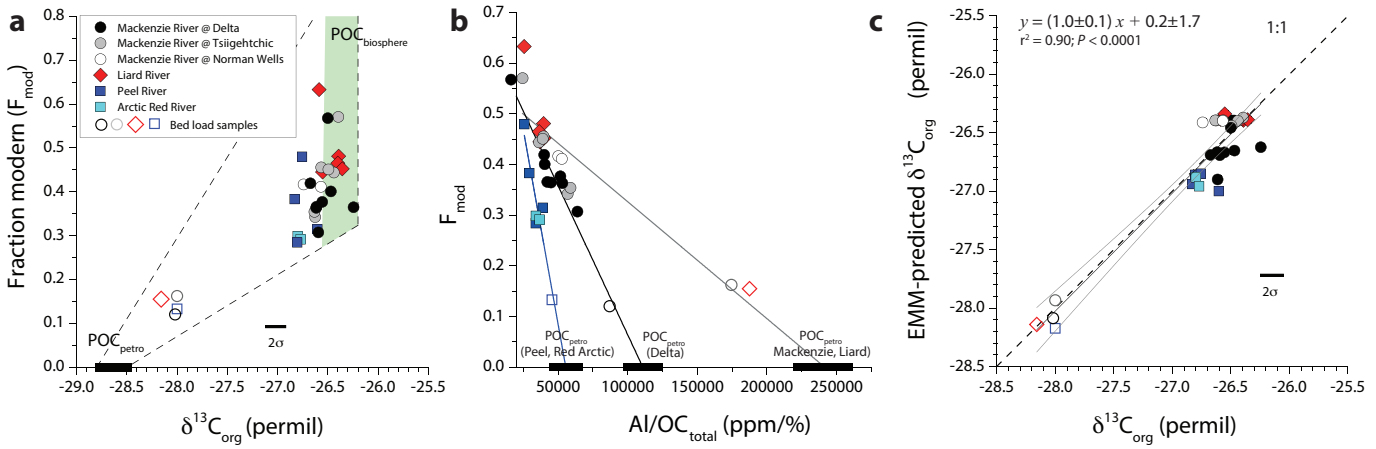

Extended Data Figure 2 | Source of particulate organic carbon in the Mackenzie River basin. **a**, Radiocarbon content (reported as F_{mod}) as a function of the stable isotope ratio of organic carbon ($\delta^{13}C_{org}$) of river sediments for the Mackenzie River (circles) and its major tributaries (diamonds and squares) for suspended load samples from river depth profiles (filled symbols) and river bed materials (open symbols). Dashed lines and shaded regions show hypothetical compositions produced by mixing rock-derived POC_{petro}[40] and $POC_{biosphere}$[41]. **b**, F_{mod} as a function of Al/OC_{total}. High Al/OC_{total} and low F_{mod} correspond to the petrogenic source of POC (POC_{petro}). Linear trends are shown for the Peel and Arctic Red rivers (blue, $y = (-1.5 \pm 0.3 \times 10^{-6})x + (0.85 \pm 0.11)$, $r^2 = 0.85$, $P < 0.02$), the Mackenzie River at delta (black, $y = (-5.9 \pm 0.5 \times 10^{-6})x + (0.65 \pm 0.03)$, $r^2 = 0.95$, $P < 0.001$), and the Mackenzie and Liard rivers (grey, $y = (-2.3 \pm 0.3 \times 10^{-6})x + (0.56 \pm 0.03)$, $r^2 = 0.82$, $P < 0.001$). The intercepts at $F_{mod} = 0$ for POC_{petro} are given with uncertainty (± 1 s.d.) and are different for each sub-basin, reflecting the distribution of organic carbon-rich rocks in the Mackenzie mountains[40]. **c**, Measured $\delta^{13}C_{org}$ versus those predicted by the endmember mixing model (EMM-predicted) (equations (1) and (2); Methods). The good agreement between measured and predicted values within the uncertainty on the measurements suggests that mixing of POC_{petro} and $POC_{biosphere}$ can explain the first-order variability in $\delta^{13}C_{org}$ values between catchments and between suspended load and river bed materials.

©2015 Macmillan Publishers Limited. All rights reserved

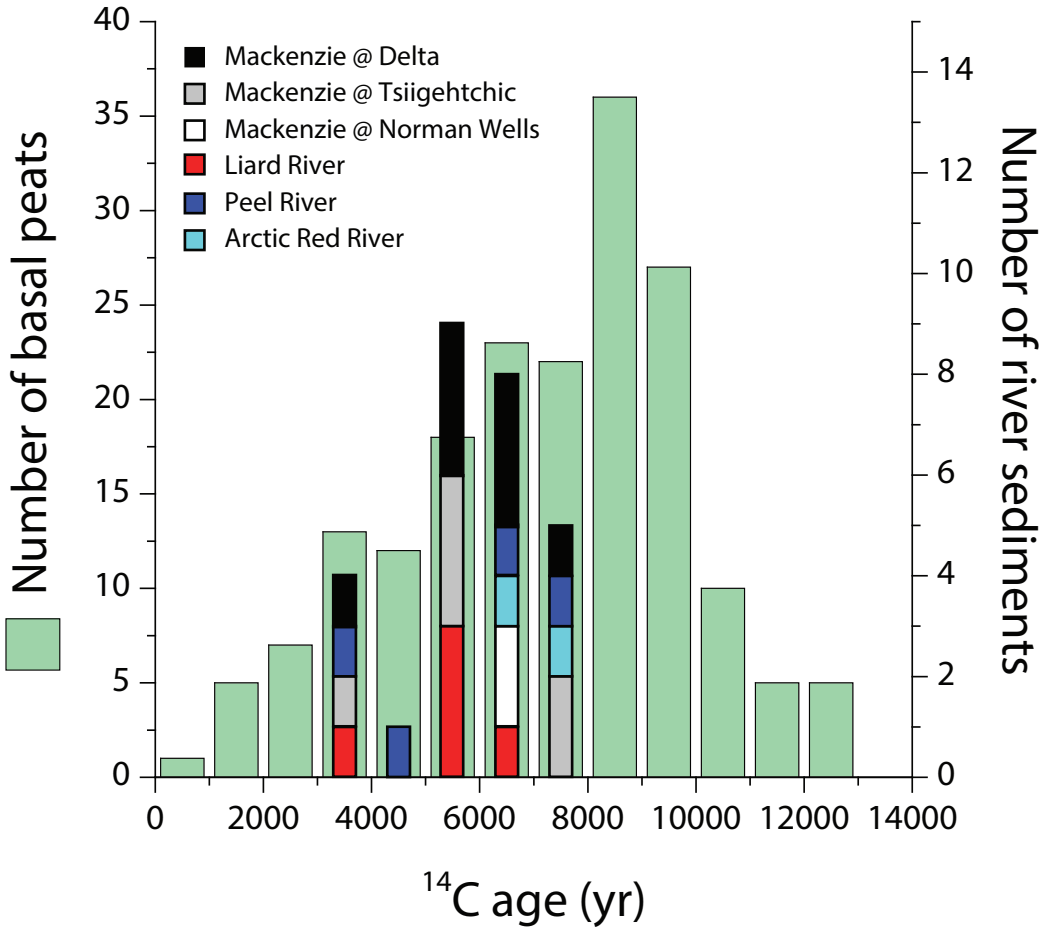

Extended Data Figure 3 | Radiocarbon age of biospheric particulate organic carbon in the Mackenzie River derived from the mixing analysis. The number of $POC_{biosphere}$ measurements of a given range of ^{14}C ages is shown for each sampling location as a narrow rectangle. The distribution of published basal peat sample ^{14}C ages for the Mackenzie River basin[25] is shown as wide rectangles.

©2015 Macmillan Publishers Limited. All rights reserved

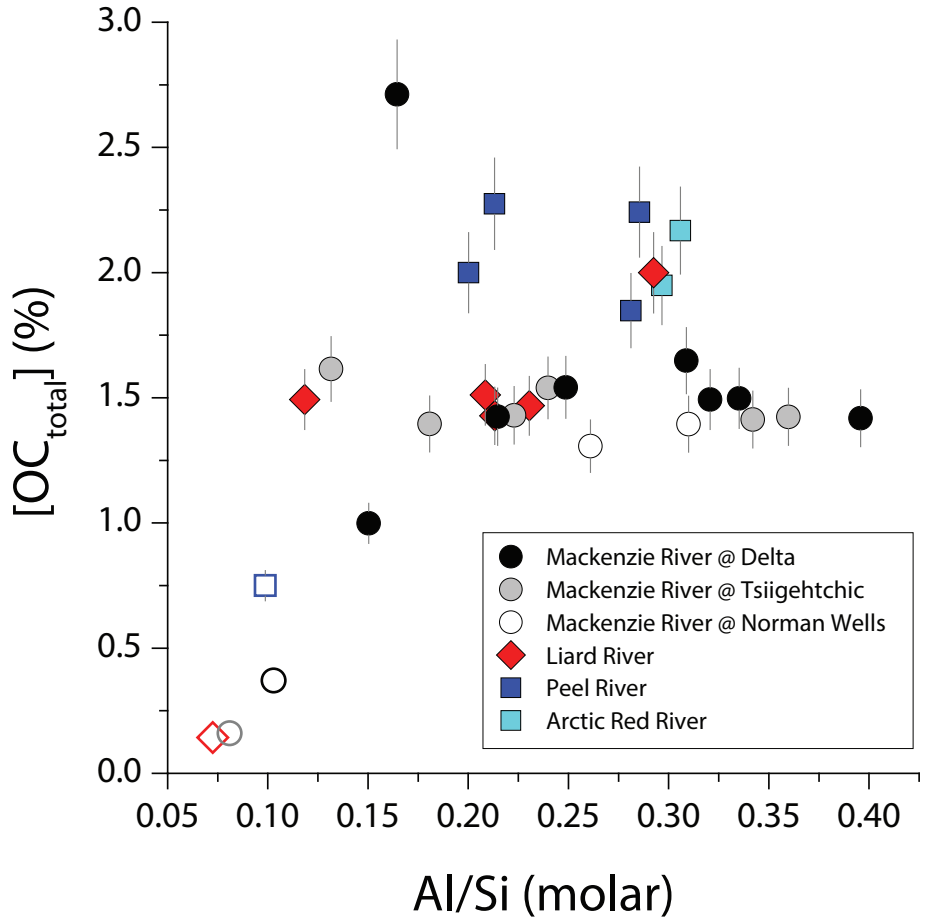

Extended Data Figure 4 | River particulate organic carbon in the Mackenzie basin. Organic carbon concentration as a function of Al/Si, which is a function of grain size in the Mackenzie River basin[26]. Analytical errors (2 s.d.) are shown as grey lines if larger than the point size.

©2015 Macmillan Publishers Limited. All rights reserved

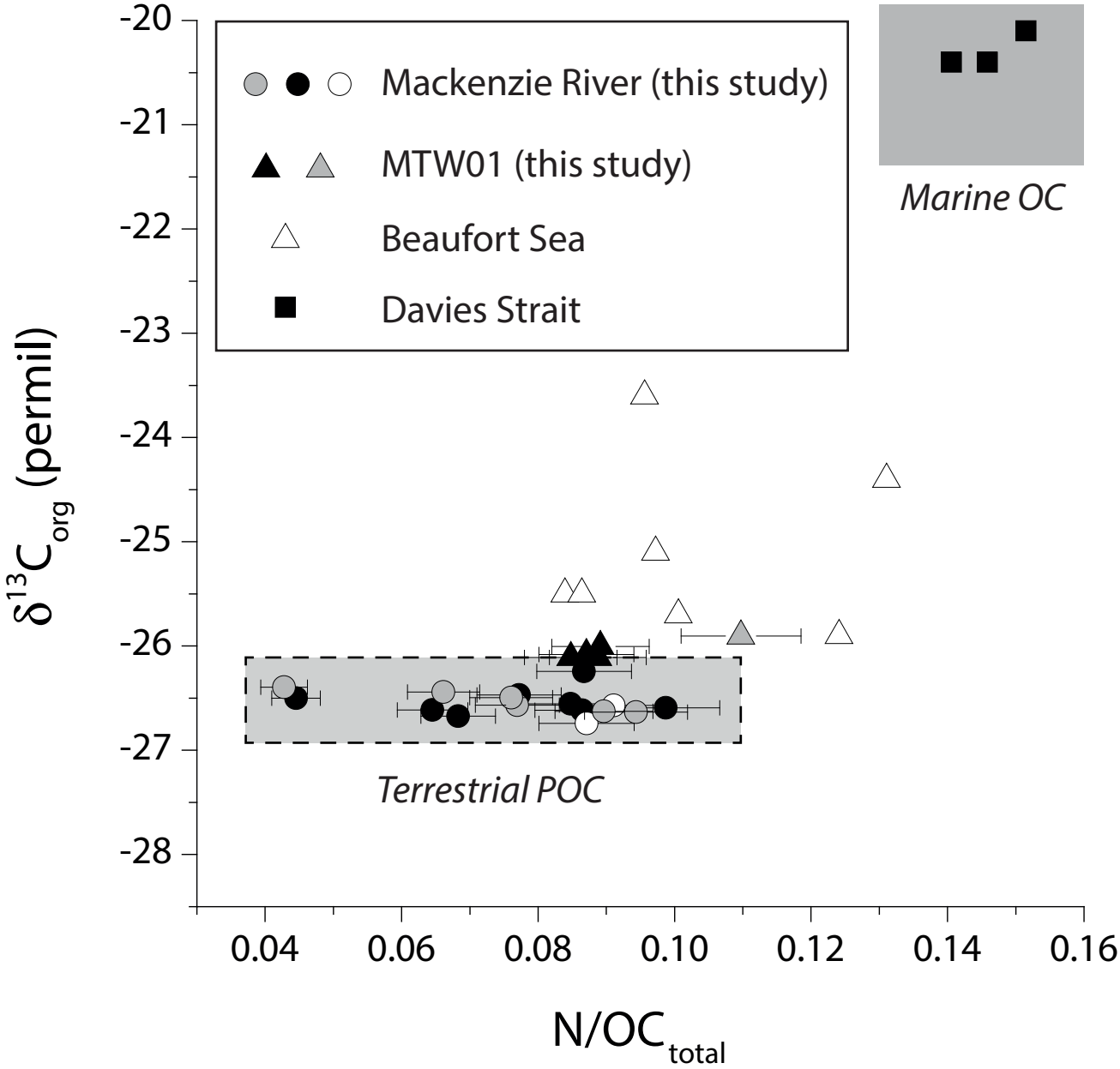

Extended Data Figure 5 | Stable isotope composition and nitrogen to organic carbon ratio of terrestrial and marine sediments. Suspended sediments from the Mackenzie River (circles) at the delta (black), Tsiigehtchic (grey) and Norman Wells (white) are shown. Marine sediment samples from the MTW01 sediment core (this study, triangles, black <63 μm, grey >63 μm) are shown with published surface sediment samples from the Beaufort Sea (white triangles) and Davis Strait (black squares)[7,29]. The terrestrial POC field shows an indicative range of values measured in the Mackenzie River. The marine OC field shows values expected for Arctic Ocean marine OC. Analytical errors (2 s.d.) are shown as grey lines if larger than the point size.

©2015 Macmillan Publishers Limited. All rights reserved

Extended Data Table 1 | River suspended sediment and bed material samples from the Mackenzie basin in 2009–2011

Sample ID	River	Location	Date	Lat.	Long.	Type[a]	Depth (m)	SSC[b] (mg/L)	Al (ppm)	Al/Si[c] (molar)	$[OC_{total}]$ (%)			$\delta^{13}C_{org}$ (permil)	N/OC_{total}			F_{mod}[d]			Publication Code
CAN10_28	Mackenzie	Delta	09/09/2010	68.4092	134.0805	SL	19	513	56947	0.21	1.42	±	0.11	-26.7	0.068	±	0.005	0.419	±	0.002	SUERC-43077
CAN10_29	Mackenzie	Delta	09/09/2010	68.4092	134.0805	SL	17	275	77165	0.32	1.49	±	0.12	-26.6	0.085	±	0.007	0.377	±	0.002	SUERC-43078
CAN10_31	Mackenzie	Delta	09/09/2010	68.4092	134.0805	SL	6	251	79441	0.34	1.50	±	0.12	-26.6	0.086	±	0.007	0.363	±	0.002	SUERC-43079
CAN10_32	Mackenzie	Delta	09/09/2010	68.4092	134.0805	SL	0	162	90608	0.40	1.42	±	0.11	-26.6	0.099	±	0.008	0.307	±	0.002	SUERC-43080
CAN11_87	Mackenzie	Delta	13/06/2011	68.4092	134.0805	SL	20	848	43833	0.16	2.71	±	0.22	-26.5	0.045	±	0.004	0.568	±	0.003	SUERC-43100
CAN11_88	Mackenzie	Delta	13/06/2011	68.4092	134.0805	SL	15	850	42155	0.15	1.00	±	0.08	-26.6	0.065	±	0.005	0.366	±	0.002	SUERC-43101
CAN11_89	Mackenzie	Delta	13/06/2011	68.4092	134.0805	SL	8	240	62214	0.25	1.54	±	0.12	-26.5	0.077	±	0.006	0.401	±	0.002	SUERC-43102
CAN11_90	Mackenzie	Delta	13/06/2011	68.4092	134.0805	SL	0	119	74070	0.31	1.65	±	0.13	-26.2	0.087	±	0.007	0.365	±	0.002	SUERC-43103
CAN10_38	Mackenzie	Delta	09/09/2010	68.4092	134.0805	BM	Thalweg	-	32258	0.10	0.37	±	0.03	-28.0	0.076	±	0.006	0.120	±	0.001	SUERC-46907
CAN09_55	Mackenzie	Tsiigehtchic	23/07/2009	67.4530	133.7405	SL	0	-	-	-	1.50		0.03	-26.6	0.104	±	0.004	0.217	±	0.001	OS-78930
CAN10_16	Mackenzie	Tsiigehtchic	07/09/2010	67.4530	133.7405	BM	Thalweg	-	27913	0.08	0.16	±	0.01	-28.0	0.063	±	0.005	0.162	±	0.001	SUERC-46902
CAN10_10	Mackenzie	Tsiigehtchic	07/09/2010	67.4530	133.7405	SL	23	255	80393	0.34	1.41	±	0.11	-26.6	0.090	±	0.007	0.342	±	0.002	SUERC-43071
CAN10_15	Mackenzie	Tsiigehtchic	07/09/2010	67.4530	133.7405	SL	0	231	83833	0.36	1.42	±	0.11	-26.6	0.094	±	0.008	0.354	±	0.002	SUERC-43072
CAN11_65	Mackenzie	Tsiigehtchic	11/06/2011	67.4530	133.7405	SL	13	941	39509	0.13	1.62	±	0.13	-26.4	0.043	±	0.003	0.570	±	0.003	SUERC-43091
CAN11_66	Mackenzie	Tsiigehtchic	11/06/2011	67.4530	133.7405	SL	10	445	50607	0.18	1.40	±	0.11	-26.4	0.066	±	0.005	0.444	±	0.002	SUERC-43092
CAN11_67	Mackenzie	Tsiigehtchic	11/06/2011	67.4530	133.7405	SL	5	322	56614	0.22	1.43	±	0.11	-26.6	0.077	±	0.006	0.456	±	0.002	SUERC-43093
CAN11_68	Mackenzie	Tsiigehtchic	11/06/2011	67.4530	133.7405	SL	0	291	59948	0.24	1.54	±	0.12	-26.5	0.076	±	0.006	0.451	±	0.002	SUERC-43097
CAN10_39	Mackenzie	Norman Wells	10/09/2010	65.2650	126.7594	SL	3.15	168	65521	0.26	1.31	±	0.10	-26.7	0.087	±	0.007	0.417	±	0.002	SUERC-43082
CAN10_40	Mackenzie	Norman Wells	10/09/2010	67.4530	126.7594	SL	0	136	73513	0.31	1.39	±	0.11	-26.6	0.091	±	0.007	0.411	±	0.002	SUERC-43083
CAN10_50	Liard	Fort Simpson	13/09/2010	61.8234	121.2976	BM	Thalweg	-	26796	0.07	0.14	±	0.01	-28.2	0.070	±	0.006	0.155	±	0.001	SUERC-46906
CAN10_46	Liard	Fort Simpson	13/09/2010	61.8234	121.2976	SL	4.8	492	38265	0.12	1.49	±	0.12	-26.6	0.045	±	0.004	0.633	±	0.003	SUERC-43086
CAN10_49	Liard	Fort Simpson	13/09/2010	61.8234	121.2976	SL	0	79	73830	0.29	2.00	±	0.16	-26.6	0.077	±	0.006	0.445	±	0.002	SUERC-43087
CAN11_03	Liard	Fort Simpson	04/06/2011	61.8234	121.2976	SL	6.5	490	56524	0.21	1.43	±	0.11	-26.4	0.075	±	0.006	0.481	±	0.002	SUERC-43088
CAN11_05	Liard	Fort Simpson	04/06/2011	61.8234	121.2976	SL	3.5	542	55058	0.21	1.51	±	0.12	-26.4	0.069	±	0.006	0.465	±	0.002	SUERC-43089
CAN11_07	Liard	Fort Simpson	04/06/2011	61.8234	121.2976	SL	0	438	58509	0.23	1.47	±	0.12	-26.4	0.073	±	0.006	0.452	±	0.002	SUERC-43090
CAN10_07	Peel	Fort McPherson	07/09/2010	67.3313	134.8656	BM	Thalweg	-	34205	0.10	0.75	±	0.06	-28.0	0.068	±	0.005	0.133	±	0.001	SUERC-46905
CAN10_03	Peel	Fort McPherson	07/09/2010	67.3313	134.8656	SL	8.5	250	58694	0.20	2.00	±	0.16	-26.8	0.071	±	0.006	0.383	±	0.002	SUERC-43069
CAN10_06	Peel	Fort McPherson	07/09/2010	67.3313	134.8656	SL	0	101	76053	0.29	2.24	±	0.18	-26.8	0.080	±	0.006	0.284	±	0.002	SUERC-43070
CAN11_77	Peel	Fort McPherson	11/06/2011	67.3313	134.8656	SL	6	325	58519	0.21	2.27	±	0.18	-26.8	0.072	±	0.006	0.480	±	0.002	SUERC-43098
CAN11_79	Peel	Fort McPherson	11/06/2011	67.3313	134.8656	SL	0	146	72153	0.28	1.85	±	0.15	-26.6	0.085	±	0.007	0.315	±	0.002	SUERC-43099
CAN10_17	Arctic Red	Tsiigehtchic	07/09/2010	67.4394	133.7529	SL	6	123	73830	0.31	2.17	±	0.17	-26.8	0.080	±	0.006	0.299	±	0.002	SUERC-43073
CAN10_19	Arctic Red	Tsiigehtchic	07/09/2010	67.4394	133.7529	SL	0	123	71608	0.30	1.95	±	0.16	-26.8	0.083	±	0.007	0.291	±	0.002	SUERC-43076

[a]River sample type: SL, suspended load; BM, bed material, collected at the thalweg (deepest part of the river channel cross-section).
[b]SSC, suspended sediment concentration.
[c]Aluminium to silicon ratio[26].
[d]F_{mod} from radiocarbon activity.

©2015 Macmillan Publishers Limited. All rights reserved

Extended Data Table 2 | Sediment samples from the offshore core MTW01

Interval	Depth (m)	Dated material	^{14}C Age (yrs)	$\delta^{13}C_{foram}$ (permil)	^{14}C Age $\delta^{13}C$ normalised (yrs)[a]	ΔR (yr)[b]	Calibrated age (cal. yrs BP)[c]	plus σ	minus σ	Publication code #	Date Reported	Grain size fraction	$[OC_{total}]$ (%)[d]			$\delta^{13}C_{org}$ (permil)	N/OC_{total}			Al (ppm)
1A	0-0.2	Mixed Benthic Foraminifera	1860 ±25	-1.4	2244±89	335± 85	1461	1548	1353	OS-103002	21/05/2013	>63µm	1.34	±	0.11	-25.7		-		-
												<63µm	1.72	±	0.14	-26.1	0.09	±	0.01	89010
6B	7.62-8.12	Mixed Benthic Foraminifera	4280 ±20	-1.6	4661±87	335± 85	4462	4590	4333	OS-103185	24/05/2013	>63µm	1.40	±	0.11	-25.8		-		-
												<63µm	1.58	±	0.13	-26.1	0.08	±	0.01	89127
12B	16.92-17.42	Mixed Benthic Foraminifera	7080 ±35	-0.9	7472±92	335± 85	7612	7689	7517	OS-95351	22/05/2012	>63µm	1.19	±	0.10	-25.9	0.11	±	0.01	80960
												<63µm	1.52	±	0.12	-26.0	0.09	±	0.01	87687
15B	20.73-21.09	Mixed Benthic Foraminifera	8490 ±70	-0.9	8882±110	335± 85	9183	9308	9027	OS-95606	04/06/2012	>63µm	1.09	±	0.09	-25.9		-		-
												<63µm	1.50	±	0.12	-26.1	0.09	±	0.01	-

[a]See Methods.
[b]Reservoir age (see Methods).
[c]Calibrated age in calibrated years before present, based on MARINE13 data set in CALIB v7.1 (Methods).
[d]Organic carbon concentration for the sediment samples.

©2015 Macmillan Publishers Limited. All rights reserved

Extended Data Table 3 | River bank samples from the Mackenzie River in 2009

Sample ID	Grain size fraction	River	Location	Date	Lat.	Long.	Type	$[OC_{total}]$ (%)			$\delta^{13}C_{org}$ (permil)	N/OC_{total}			F_{mod}			Publication Code
CAN09-54	150-250µm	Mackenzie	Tsiigehtchic	23/07/2009	67.45384	133.70741	Flood dep.	2.02	±	0.11	-26.7	0.052	±	0.003	0.672	±	0.003	OS-78930
CAN09-54	63-150µm	Mackenzie	Tsiigehtchic	23/07/2009	67.45384	133.70741	Flood dep.	1.01	±	0.03	-27.0	0.069	±	0.002	0.444	±	0.002	OS-78929
CAN09-54	<63µm	Mackenzie	Tsiigehtchic	23/07/2009	67.45384	133.70741	Flood dep.	1.06	±	0.05	-27.0	0.098	±	0.005	0.371	±	0.001	OS-78928
CAN09-54	Bulk	Mackenzie	Tsiigehtchic	23/07/2009	67.45384	133.70741	Flood dep.	0.99	±	0.00	-26.9	0.085	±	0.002	0.455	±	0.002	OS-78927
CAN09-12	150-250µm	Liard	Fort Simpson	16/07/2009	61.84457	121.31625	Flood dep.	17.47	±	1.24	-26.6	0.044	±	0.003	0.839	±	0.003	OS-79575
CAN09-12	63-150µm	Liard	Fort Simpson	16/07/2009	61.84457	121.31625	Flood dep.	0.84	±	0.01	-26.6	0.087	±	0.001	0.403	±	0.002	OS-79574
CAN09-12	<63µm	Liard	Fort Simpson	16/07/2009	61.84457	121.31625	Flood dep.	0.66	±	0.02	-26.6	0.132	±	0.006	0.364	±	0.002	OS-79573
CAN09-12	Bulk	Liard	Fort Simpson	16/07/2009	61.84457	121.31625	Flood dep.	1.04	±	0.06	-26.7	0.069	±	0.004	0.523	±	0.002	OS-79576
CAN09-42	<63µm	Peel	Fort McPherson	22/07/2009	67.33189	134.86912	Flood dep.	1.63	±	0.10	-27.1	0.089	±	0.005	0.328	±	0.002	OS-78922
CAN09-42	Bulk	Peel	Fort McPherson	22/07/2009	67.33189	134.86912	Flood dep.	2.01	±	0.04	-27.1	0.082	±	0.002	0.440	±	0.002	OS-78921

©2015 Macmillan Publishers Limited. All rights reserved